Biophysical Journal, Volume *116*

Supplemental Information

Convection-Induced Biased Distribution of Actin Probes in Live Cells

Sawako Yamashiro, Daisuke Taniguchi, Soichiro Tanaka, Tai Kiuchi, Dimitrios Vavylonis, and Naoki Watanabe

Supplementary Table S1

Model parameters

Symbol	Description	Value
v	Retrograde flow speed relative to cell migration speed	
	XTC cell	60 nm s^{-1}
	keratocyte	100 nm s^{-1}
D	Diffusion coefficient of free actin probe	
	Lifeact-mCherry	6.8 μm^2 s^{-1}
	Alexa647-phalloidin	16.7 μm^2 s^{-1}
k_{on}	Probe association rate	
	Lifeact-mCherry	2.28 $\mu M^{-1} s^{-1}$
	Alexa647-phalloidin	2.9×10^{-2} $\mu M^{-1} s^{-1}$
k_{off}	Probe dissociation rate	
	Lifeact-mCherry	30.1 s^{-1}
	Alexa647-phalloidin	0.08 s^{-1}
$\bar{F}$	Uniform F-actin concentration	1000 μM
a	Slope of non-uniform F-actin concentration	112.5 μM μm^{-1}
b	Base of non-uniform F-actin concentration	100 μM
L	Lamellipodium length	8 μm

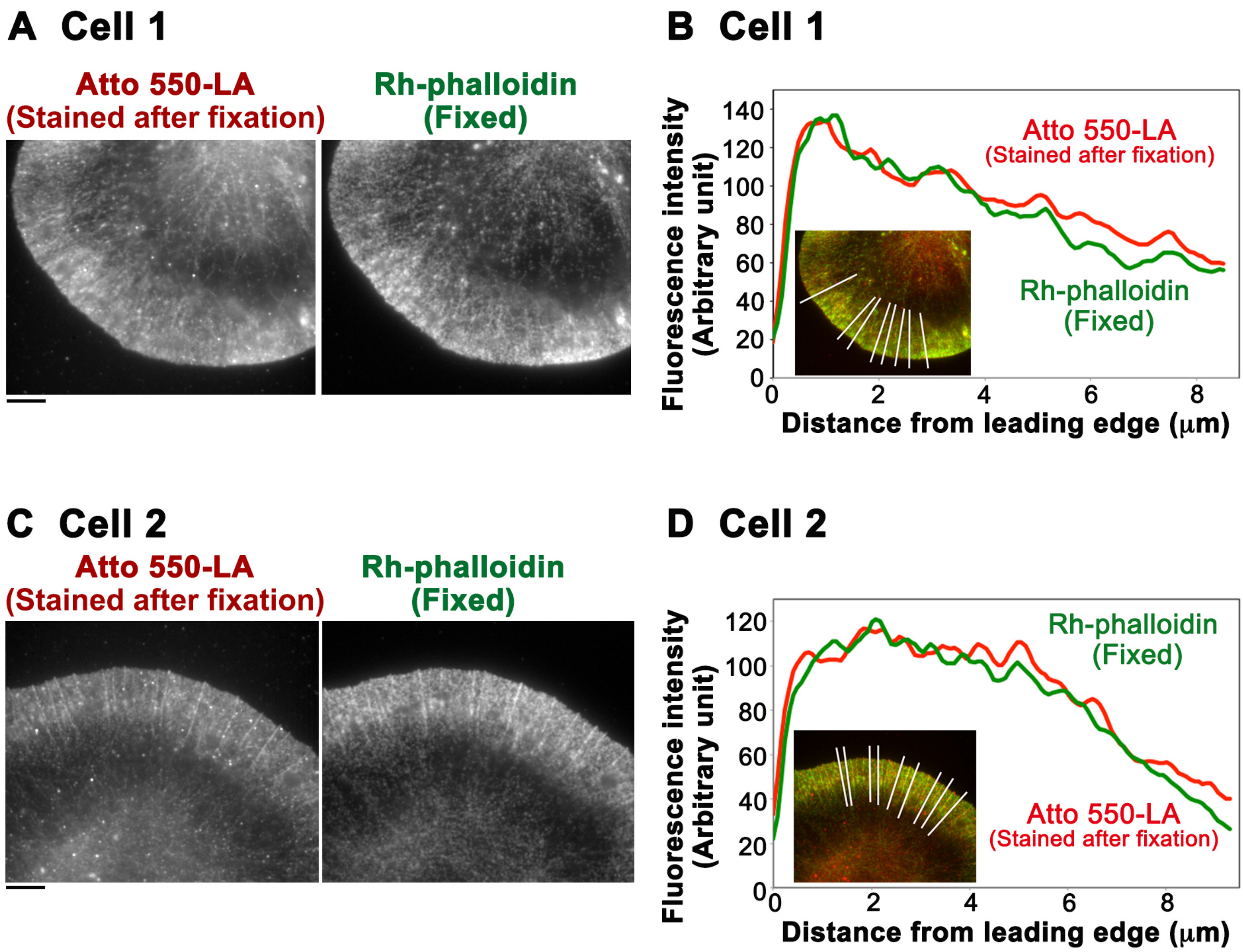

Suppl. Fig. S1

Figure S1. Two other examples of the experiments in Fig. 1 ***D*** and ***E***. The data show similar distribution of Atto 550-Lifeact (Atto 550-LA) and rhodamine-phalloidin (Rh-phalloidin) in fixed XTC cells.
(*A*, and *C*) Images of fixed cells stained with Atto 550-LA (left) and Rh-phalloidin (right). Bars = 5 µm.
(*B*, and *D*) Average fluorescence intensity of the images in *A* or *C* along the white lines in the insets.

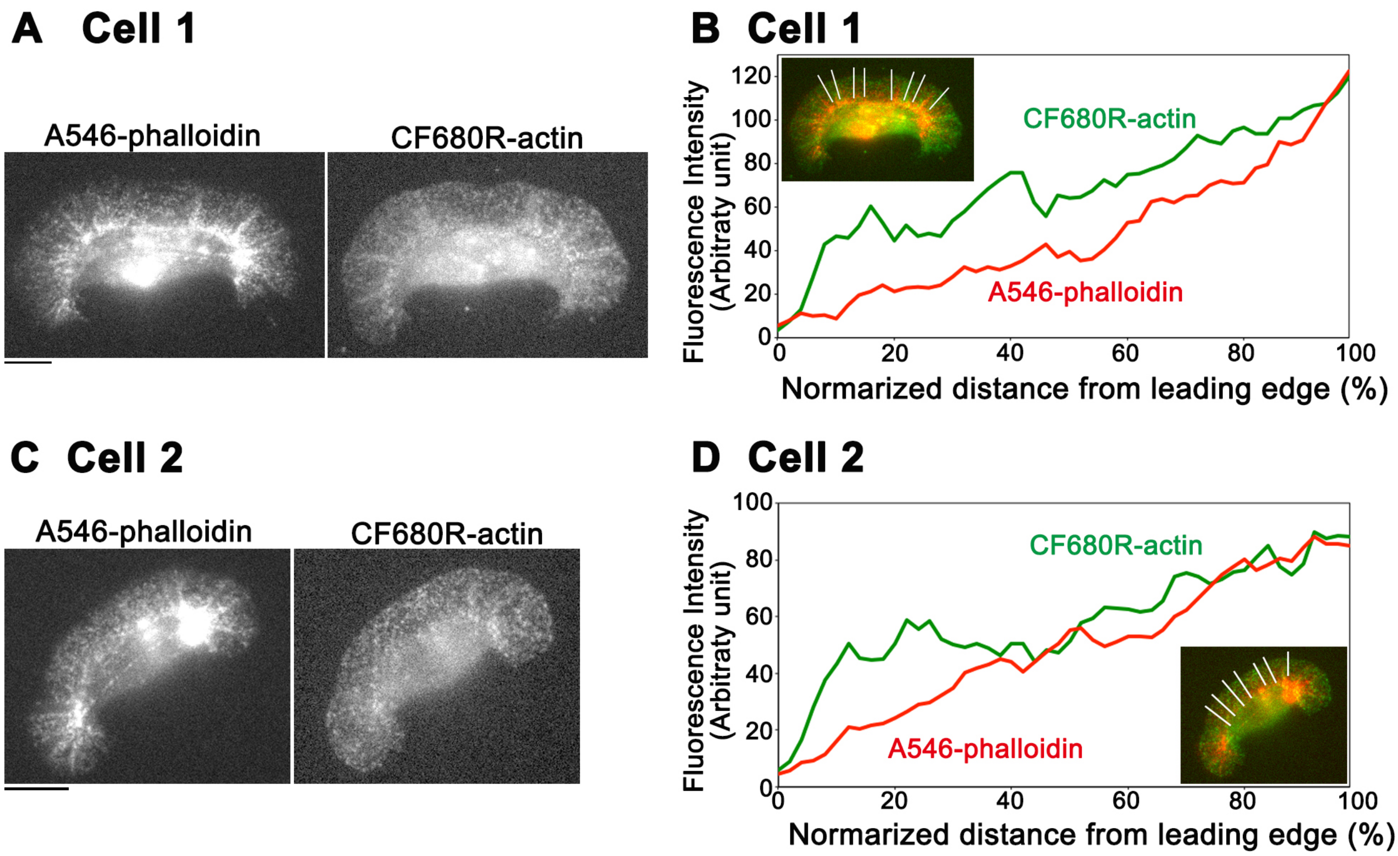

Suppl. Fig. S2

Figure S2. Two other examples of the experiments in Fig. 2. **(*A*, and *C*)** Fluorescent speckle images of Alexa546-phalloidin (A546-phalloidin, left) and CF680R-actin (right) in live fish keratocytes. Bars = 10 µm. **(*B*, and *D*)** Average fluorescence intensity of the images in *A* or *C* along the white lines in the insets.

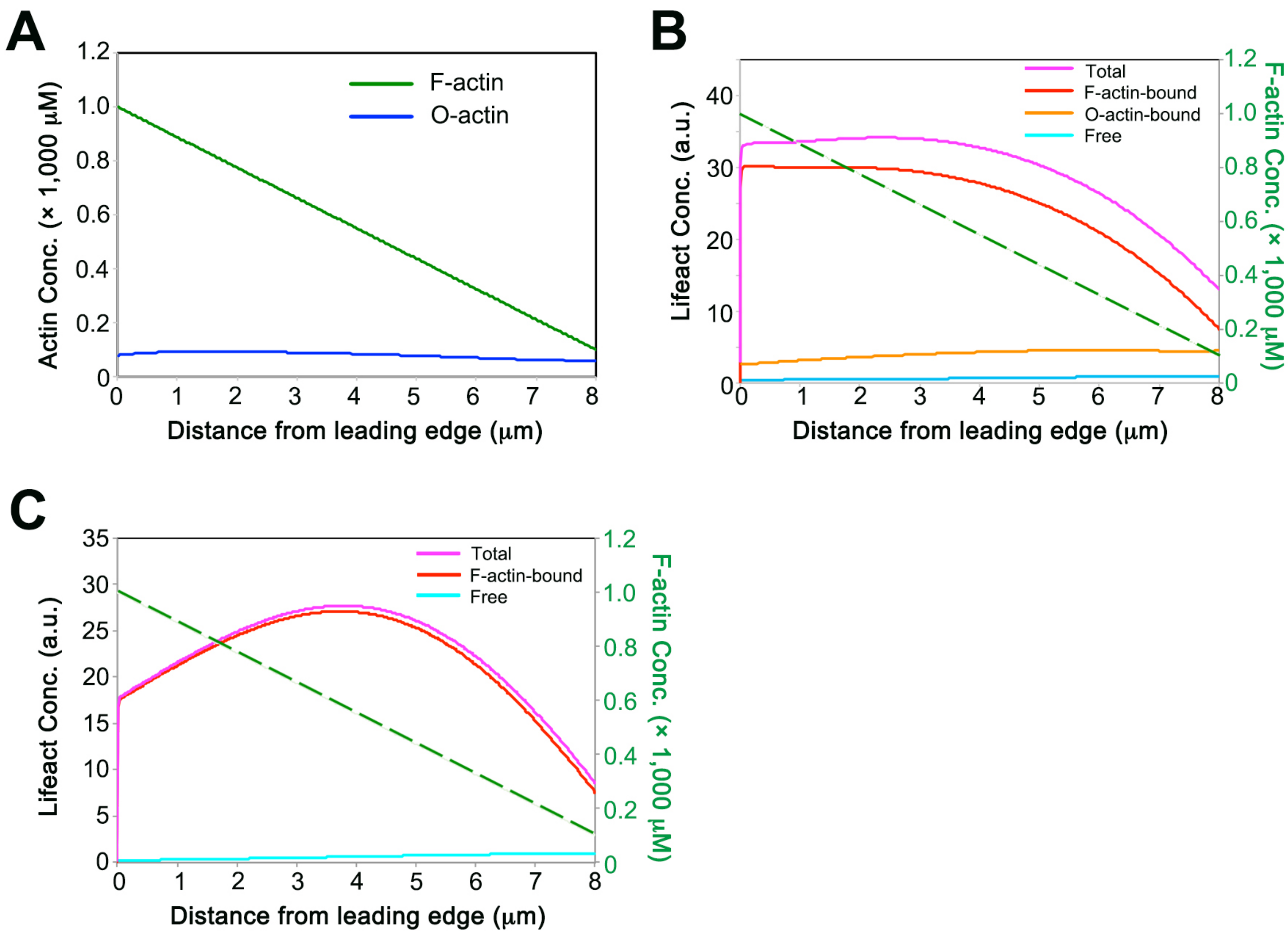

Suppl. Fig. S3

Figure S3. Simulated concentration profile of Lifeact-mCherry in a model with both F-actin and actin oligomers (O-actin) as Lifeact-binding species. ***(A)*** Concentration profiles of F- and O-actin in lamellipodia. The ratio of O-actin to F-actin is set as ~0.1 at leading edge (29). ***(B)*** Calculated distributions of Lifeact-mCherry in the states of F-actin-bound (red), O-actin-bound (orange) and free (light blue). The distribution of total Lifeact-mCherry is indicated by the pink line. A model lamellipodium with a linear decrease in F-actin concentration is indicated in a green dotted line. The supplementary method of simulation including oligomer actin is described below. ***(C)*** Calculated distribution of Lifeact-mCherry in a model with F-actin as only Lifeact-binding species. The method and the model parameters for simulation is same to that used in Fig. 3 ***C***, except for the retrograde flow speed was set as 30 nm/s.

[Supplementary method of simulation including oligomer actin employed in Fig. S3***B***]

1 Model equations

The modified model to take into account the effect of oligomer actin is as follows

$$\frac{\partial C_{\mathrm{f}}}{\partial t} = D_{\mathrm{f}}\frac{\partial^2 C_{\mathrm{f}}}{\partial x^2} + k_{\mathrm{off}}C_{\mathrm{fb}} - k_{\mathrm{on}}FC_{\mathrm{f}} + k_{-}C_{\mathrm{ob}} - k_{+}OC_{\mathrm{f}} + k_{\mathrm{d}}C_{\mathrm{ob}} \quad (1)$$

$$\frac{\partial C_{\mathrm{fb}}}{\partial t} = v\frac{\partial C_{\mathrm{fb}}}{\partial x} - k_{\mathrm{off}}C_{\mathrm{fb}} + k_{\mathrm{on}}FC_{\mathrm{f}} - k_{\mathrm{s}}C_{\mathrm{fb}} + k_{\mathrm{i}}FC_{\mathrm{ob}} \quad (2)$$

$$\frac{\partial C_{\mathrm{ob}}}{\partial t} = D_{\mathrm{o}}\frac{\partial^2 C_{\mathrm{ob}}}{\partial x^2} + k_{\mathrm{s}}C_{\mathrm{fb}} - k_{\mathrm{i}}FC_{\mathrm{ob}} - k_{-}C_{\mathrm{ob}} + k_{+}OC_{\mathrm{f}} - k_{\mathrm{d}}C_{\mathrm{ob}} \quad (3)$$

$$\frac{\partial O}{\partial t} = D_{\mathrm{o}}\frac{\partial^2 O}{\partial x^2} + k_{\mathrm{s}}F - k_{\mathrm{i}}FO - k_{\mathrm{d}}O \quad (4)$$

where C_{f}, C_{fb}, and C_{ob} are respectively the concentration of free, F-actin-bound, oligomer actin-bound probes. F and O represent the concentration of F-actin and oligomer actin at 1-dimensional position x at time t, respectively. x ranges from 0 (lamellipodial base) from L (leading edge). Based on our experimental data of $F(x)$ in XTC cells, we assumed that the concentration profile of actin, $F(x)$, is prescribed as $F(x) = ax + b$. The model parameters are summarized in Supplementary Table S2.

Supplementary Table S2: Model parameters for Fig. S3B

Symbol	Meaning	Value
v	Retrograde flow speed	30 nm s^{-1}
D_{f}	Diffusion coefficient of free Lifeact	6.8 μm^2 s^{-1}
D_{o}	Diffusion coefficient of oligomer actin	1.0 μm^2 s^{-1}
k_{on}	Rate at which free Lifeact associates with F-actin	2.28 μM^{-1} s^{-1}
k_{off}	Rate at which F-actin-bound Lifeact dissociates from F-actin	30.1 s^{-1}
k_{+}	Rate at which free Lifeact associates with O-actin	2.28 μM^{-1} s^{-1}

k_-	Rate at which O-actin-bound Lifeact dissociates from O-actin	30.1 s^{-1}
k_s	F-actin severing rate	0.25 s^{-1}
k_i	Rate at which O-actin is incorporated into F-actin	0.002 μM^{-1} s^{-1}
k_d	Disassembly rate of O-actin	0.5 s^{-1}
a	Slope of linear F-actin concentration profile	112.5 μM μm^{-1}
b	Base of linear F-actin concentration profile	100 μM
L	Lamellipodial length	8 μm

The boundary conditions at the steady state are

$$C_f(0) = \text{const.}, \frac{\partial C_f(L)}{\partial x} = 0 \quad (5)$$
$$vC_{fb}(L) = 0 \quad (6)$$
$$D_o \frac{\partial C_{ob}(0)}{\partial x} = -vC_{fb}(0), D_o \frac{\partial C_{ob}(L)}{\partial x} = -vC_{fb}(L) \quad (7)$$
$$D_o \frac{\partial O(0)}{\partial x} = -vF(0), D_o \frac{\partial O(L)}{\partial x} = -vF(L) \quad (8)$$

In Eq. (5), const. is determined by the total amount of the probe.

2 Spatial discretization

Using the standard finite difference scheme, Eqs. (1)-(4) with the boundary conditions Eqs. (5)-(8) in the steady-state are discretized in space with a step Δx as

$$0 = D_\mathrm{f}\frac{C_\mathrm{f}(x_{i+1}) - 2C_\mathrm{f}(x_i) + C_\mathrm{f}(x_{i-1})}{\Delta x^2} + k_\mathrm{off}C_\mathrm{fb}(x_i) - k_\mathrm{on}F(x_i)C_\mathrm{f}(x_i) + k_-C_\mathrm{ob}(x_i) - k_+O(x_i)C_\mathrm{f}(x_i) + k_\mathrm{d}C_\mathrm{ob}(x_i) \quad (2 \le i \le n-1) \tag{9}$$
$$C_\mathrm{f}(x_1) = \text{const.} \tag{10}$$
$$C_\mathrm{f}(x_n) = C_\mathrm{f}(x_{n-1}) \tag{11}$$
$$0 = v\frac{C_\mathrm{fb}(x_{i+1}) - C_\mathrm{fb}(x_i)}{\Delta x} - k_\mathrm{off}C_\mathrm{fb}(x_i) + k_\mathrm{on}F(x_i)C_\mathrm{f}(x_i) - k_\mathrm{s}C_\mathrm{fb}(x_i) + k_\mathrm{i}F(x_i)C_\mathrm{ob}(x_i) \quad (1 \le i \le n-1) \tag{12}$$
$$C_\mathrm{fb}(x_n) = 0 \tag{13}$$
$$0 = D_\mathrm{o}\frac{C_\mathrm{ob}(x_{i+1}) - 2C_\mathrm{ob}(x_i) + C_\mathrm{ob}(x_{i-1})}{\Delta x^2} + k_\mathrm{s}C_\mathrm{fb}(x_i) - k_\mathrm{i}F(x_i)C_\mathrm{ob}(x_i) - k_-C_\mathrm{ob}(x_i) + k_+O(x_i)C_\mathrm{f}(x_i) - k_\mathrm{d}C_\mathrm{ob}(x_i) \quad (2 \le i \le n-1) \tag{14}$$
$$C_\mathrm{ob}(x_1) = C_\mathrm{ob}(x_2) + \frac{v\Delta x}{D_\mathrm{o}}C_\mathrm{fb}(x_1) \tag{15}$$
$$C_\mathrm{ob}(x_n) = C_\mathrm{ob}(x_{n-1}) - \frac{v\Delta x}{D_\mathrm{o}}C_\mathrm{fb}(x_n) \tag{16}$$
$$0 = D_\mathrm{o}\frac{O(x_{i+1}) - 2O(x_i) + O(x_{i-1})}{\Delta x^2} + k_\mathrm{s}F(x_i) - k_\mathrm{i}F(x_i)O(x_i) - k_\mathrm{d}O(x_i) \quad (2 \le i \le n-1) \tag{17}$$
$$O(x_1) = O(x_2) + \frac{v\Delta x}{D_\mathrm{o}}F(x_1) \tag{18}$$
$$O(x_n) = O(x_{n-1}) - \frac{v\Delta x}{D_\mathrm{o}}F(x_n) \tag{19}$$

where $x_i = (i-1)\Delta x \ (i = 1, \cdots, n)$ and $(n-1)\Delta x = L$. In the present study, we set $\Delta x = 0.01$ [μm].

Rearranging Eqs. (9)-(19) gives

$$C_\mathrm{f}(x_i) = \frac{C_\mathrm{f}(x_{i+1}) + C_\mathrm{f}(x_{i-1}) + c_3C_\mathrm{fb}(x_i) + c_4C_\mathrm{ob}(x_i)}{c_1F(x_i) + c_2O(x_i) + 2} \quad (2 \le i \le n-1) \tag{20}$$
$$C_\mathrm{f}(x_1) = \text{const.} \tag{21}$$
$$C_\mathrm{f}(x_n) = C_\mathrm{f}(x_{n-1}) \tag{22}$$
$$C_\mathrm{fb}(x_i) = \frac{1}{c_5}\left[C_\mathrm{fb}(x_{i+1}) + c_6F(x_i)C_\mathrm{f}(x_i) + c_7F(x_i)C_\mathrm{ob}(x_i)\right] \quad (1 \le i \le n-1) \tag{23}$$
$$C_\mathrm{fb}(x_n) = 0 \tag{24}$$
$$C_\mathrm{ob}(x_i) = \frac{C_\mathrm{ob}(x_{i+1}) + C_\mathrm{ob}(x_{i-1}) + c_{10}C_\mathrm{fb}(x_i) + c_{11}O(x_i)C_\mathrm{f}(x_i)}{c_8F(x_i) + c_9} \quad (2 \le i \le n-1) \tag{25}$$
$$C_\mathrm{ob}(x_1) = C_\mathrm{ob}(x_2) + c_{13}C_\mathrm{fb}(x_1) \tag{26}$$
$$C_\mathrm{ob}(x_n) = C_\mathrm{ob}(x_{n-1}) \tag{27}$$
$$O(x_i) = \frac{O(x_{i+1}) + O(x_{i-1}) + c_{10}F(x_i)}{c_8F(x_i) + c_{12}} \quad (2 \le i \le n-1) \tag{28}$$
$$O(x_1) = O(x_2) + c_{13}F(x_1) \tag{29}$$
$$O(x_n) = O(x_{n-1}) - c_{13}F(x_n) \tag{30}$$

where

$$c_1 = \frac{k_\mathrm{on}\Delta x^2}{D_\mathrm{f}}, c_2 = \frac{k_+\Delta x^2}{D_\mathrm{f}}, c_3 = \frac{k_\mathrm{off}\Delta x^2}{D_\mathrm{f}}, c_4 = \frac{(k_- + k_\mathrm{d})\Delta x^2}{D_\mathrm{f}}, c_5 = 1 + \frac{(k_\mathrm{off} + k_\mathrm{s})\Delta x}{v} \tag{31}$$
$$c_6 = \frac{k_\mathrm{on}\Delta x}{v}, c_7 = \frac{k_\mathrm{i}\Delta x}{v}, c_8 = \frac{k_\mathrm{i}\Delta x^2}{D_\mathrm{o}}, c_9 = 2 + \frac{(k_- + k_\mathrm{d})\Delta x^2}{D_\mathrm{o}}, c_{10} = \frac{k_\mathrm{s}\Delta x^2}{D_\mathrm{o}} \tag{32}$$
$$c_{11} = \frac{k_+\Delta x^2}{D_\mathrm{o}}, c_{12} = 2 + \frac{k_\mathrm{d}\Delta x^2}{D_\mathrm{o}}, c_{13} = \frac{v\Delta x}{D_\mathrm{o}} \tag{33}$$

Notice that Eqs. (20)-(30) remain unsolved with respect to $C_\mathrm{f}(x_i), C_\mathrm{fb}(x_i), C_\mathrm{ob}(x_i)$ and $O(x_i)$ because the RHS of Eqs. (20)-(30) also include unknown $C_\mathrm{f}(x_{i+1}), C_\mathrm{f}(x_{i-1}), C_\mathrm{fb}(x_{i+1}), C_\mathrm{ob}(x_{i+1}), C_\mathrm{ob}(x_{i-1}), O(x_{i-1})$ and $O(x_{i-1})$.

3 Iterative method to obtain the steady-state solution

To fully solve Eqs. (20)-(30), we used the following iterative update of $C_\mathrm{f}(x_i), C_\mathrm{fb}(x_i), C_\mathrm{ob}(x_i)$, and $O(x_i)$:

$$C_\mathrm{f}^{[k+1]}(x_i) \leftarrow \frac{C_\mathrm{f}^{[k]}(x_{i+1}) + C_\mathrm{f}^{[k]}(x_{i-1}) + c_3 C_\mathrm{fb}^{[k]}(x_i) + c_4 C_\mathrm{ob}^{[k]}(x_i)}{c_1 F(x_i) + c_2 O^{[k]}(x_i) + 2} \quad (2 \le i \le n-1) \tag{34}$$

$$C_\mathrm{f}^{[k+1]}(x_n) \leftarrow C_\mathrm{f}^{[k+1]}(x_{n-1}) \tag{35}$$

$$C_\mathrm{fb}^{[k+1]}(x_i) \leftarrow \frac{1}{c_5}\left[C_\mathrm{fb}^{[k]}(x_{i+1}) + c_6 F(x_i) C_\mathrm{f}^{[k]}(x_i) + c_7 F(x_i) C_\mathrm{ob}^{[k]}(x_i)\right] \quad (1 \le i \le n-1) \tag{36}$$

$$C_\mathrm{ob}^{[k+1]}(x_i) \leftarrow \frac{C_\mathrm{ob}^{[k]}(x_{i+1}) + C_\mathrm{ob}^{[k]}(x_{i-1}) + c_{10} C_\mathrm{fb}^{[k]}(x_i) + c_{11} O^{[k]}(x_i) C_\mathrm{f}^{[k]}(x_i)}{c_8 F(x_i) + c_9} \quad (2 \le i \le n-1) \tag{37}$$

$$C_\mathrm{ob}^{[k+1]}(x_1) \leftarrow C_\mathrm{ob}^{[k+1]}(x_2) + c_{13} C_\mathrm{fb}^{[k+1]}(x_1) \tag{38}$$

$$C_\mathrm{ob}^{[k+1]}(x_n) \leftarrow C_\mathrm{ob}^{[k+1]}(x_{n-1}) \tag{39}$$

$$O^{[k+1]}(x_i) \leftarrow \frac{O^{[k]}(x_{i+1}) + O^{[k]}(x_{i-1}) + c_{10} F(x_i)}{c_8 F(x_i) + c_{12}} \quad (2 \le i \le n-1) \tag{40}$$

$$O^{[k+1]}(x_1) \leftarrow O^{[k+1]}(x_2) + c_{13} F(x_1) \tag{41}$$

$$O^{[k+1]}(x_n) \leftarrow O^{[k+1]}(x_{n-1}) - c_{13} F(x_n) \tag{42}$$

where the superscript $[k]$ indicates the number of iteration steps. It is clear that one can obtain the steady-state solution of Eqs. (1)-(4) after the convergence of the loop with respect to k. During the iterations, we kept $C_\mathrm{f}(x_1)$ constant, namely, 1, and also maintained $C_\mathrm{fb}(x_n) = 0$. We set the initial guess of $C_\mathrm{f}, C_\mathrm{fb}, C_\mathrm{ob}$, and O as $C_\mathrm{f}(x_1) = 1, C_\mathrm{f}(x_{2\sim n}) = 0, C_\mathrm{fb}(x_{1\sim n}) = 0, O(x_1) = O(x_2) + c_{13}F(x_1), O(x_{2\sim n-1}) = k_\mathrm{s}F(x_{2\sim n-1})/[k_\mathrm{i}F(x_{2\sim n-1}) + k_\mathrm{d}]$, and $O(x_n) = O(x_{n-1}) - c_{13}F(x_n)$. We judged convergence of the loop if all of the following conditions are satisfied: $\| C_\mathrm{f}^{[k+1]} - C_\mathrm{f}^{[k]} \|^2 \le \epsilon$, $\|$

$C_{\mathrm{fb}}^{[k+1]} - C_{\mathrm{fb}}^{[k]} \|^2 \leq \epsilon, \| C_{\mathrm{ob}}^{[k+1]} - C_{\mathrm{ob}}^{[k]} \|^2 \leq \epsilon$ and $\| O^{[k+1]} - O^{[k]} \|^2 \leq \epsilon$ ($\epsilon = 10^{-10}$). After the convergence, we normalized $C_{\mathrm{f}}, C_{\mathrm{fb}}$ and C_{ob} such that they satisfy $\int_0^L (C_{\mathrm{f}} + C_{\mathrm{fb}} + C_{\mathrm{ob}}) dx = C_{\mathrm{tot}}$ where C_{tot} is the total amount of actin probes in lamellipodia. In the present study, we set $C_{\mathrm{tot}} = 1$.

Instead of Eq. (12) where the forward finite difference scheme was used, one might use the central finite difference scheme to replace Eq. (36) with

$$C_{\mathrm{fb}}^{[k+1]}(x_i) \quad \leftarrow \frac{1}{c_5 - 1}\left[C_{\mathrm{fb}}^{[k]}(x_{i+1}) - C_{\mathrm{fb}}^{[k]}(x_{i-1}) + c_6 F(x_i) C_{\mathrm{f}}^{[k]}(x_i) + c_7 F(x_i) C_{\mathrm{ob}}^{[k]}(x_i)\right] \quad (43)$$

However, we found that iterative updating using Eq.(43) was unstable because the RHS of Eq (43) can sometimes become negative due to $-C_{\mathrm{fb}}^{[k]}(x_{i-1})$ depending on model parameters and shape of $C_{\mathrm{fb}}(x_i)$. To ensure positivity of C_{fb} during all updating steps, we used the forward difference scheme.

A Appendix: analytical solution

In the special case where $k_{\mathrm{i}} = 0$ is satisfied, the analytical solution of O can be obtained. we used the analytical solution to check the validity of the iterative method. The steady-state model equation about O-actin and its BCs are

$$\frac{\partial^2 O}{\partial x^2} + k_{\mathrm{s}} F - k_{\mathrm{i}} F O - k_{\mathrm{d}} O = 0 \quad (44)$$

$$D_{\mathrm{o}} \frac{\partial O(0)}{\partial x} = -vF(0), D_{\mathrm{o}} \frac{\partial O(L)}{\partial x} = -vF(L), F(x) = ax + b \quad (45)$$

The solution of which is given by

$$O(x) = \frac{k_\mathrm{s}}{k_\mathrm{d}}(ax+b) + C_1 \exp\left(-\frac{x}{\lambda}\right) + C_2 \exp\left(\frac{x}{\lambda}\right) \tag{46}$$

$$C_1 = \frac{\lambda}{\exp\left(-\frac{2L}{\lambda}\right) - 1}\left\{\left(\frac{ak_\mathrm{s}}{k_\mathrm{d}} + \frac{bv}{D_\mathrm{o}}\right)\left[\exp\left(-\frac{L}{\lambda}\right) - 1\right] + \frac{avL}{D_\mathrm{o}}\exp\left(-\frac{L}{\lambda}\right)\right\} \tag{47}$$

$$C_2 = C_1 - \frac{ak_\mathrm{s}\lambda}{k_\mathrm{d}} - \frac{bv\lambda}{D_\mathrm{o}} \tag{48}$$

where $\lambda = \sqrt{D_\mathrm{o}/k_\mathrm{d}}$.

Supplementary Figure S4 compares the numerical solution and analytical solution at $D_\mathrm{o} = 0.25$ [$\mu\mathrm{m}^2\mathrm{s}^{-1}$]. The numerical solution agrees well with the analytical one.

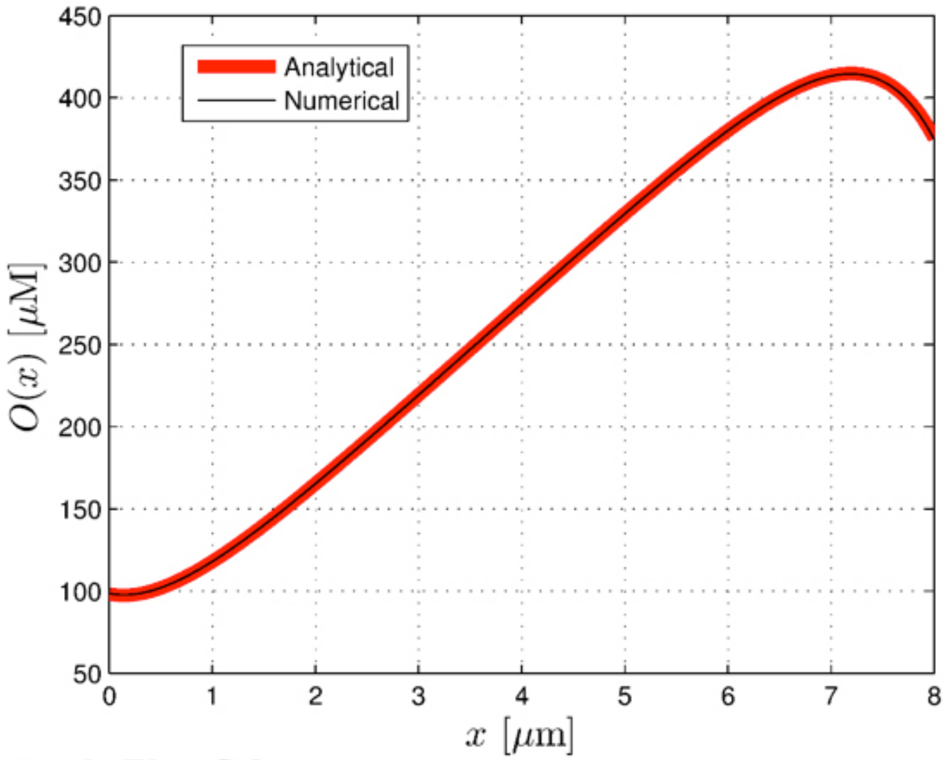

Suppl. Fig. S4

Figure S4 Comparison between analytical and numerical solutions. $D_\mathrm{o} = 0.25$ [$\mu\mathrm{m}^2\mathrm{s}^{-1}$] and $k_\mathrm{i} = 0$ [$\mu\mathrm{M}^{-1}\ \mathrm{s}^{-1}$].